Metathesis Cascade-Triggered Depolymerization of Enyne Self-Immolative Polymers

Jingsong Yuan, Gavin J. Giardino, and Jia Niu*

[a] Dr. Jingsong Yuan, Gavin J. Giardino, Prof. Dr. Jia Niu
Department of Chemistry
Boston College
Chestnut Hill, Massachusetts 02467, United States,
E-mail: jia.niu@bc.edu

Abstract: A novel class of enyne self-immolative polymers (SIPs) capable of metathesis cascade-triggered depolymerization is reported. Studies on model compounds established 1,6-enyne structures for efficient metathesis cascade reactions. SIPs incorporating the optimized 1,6-enyne motif were prepared via both polycondensation and iterative exponential growth approaches. These SIPs demonstrated excellent stability in strong acid, base, and nucleophiles, and can undergo efficient and complete depolymerization once triggered by a metathesis catalyst. Further studies revealed that introducing a terminal alkene to the chain end of the enyne SIPs improved the depolymerization efficiency, and established their potential as stimuli-responsive materials.

Self-immolative polymers (SIPs) that can undergo head-to-tail depolymerization in response to external stimuli are promising materials for a wide range of emerging applications such as recyclable plastics, drug delivery, and biosensing.[1] Compared to traditional degradable or compostable polymers (*e.g.*, polyesters and polycarbonates) that degrade in a gradual, non-controlled fashion, in principle, SIPs should be stable throughout their life cycle until being triggered by the appropriate stimulus to undergo depolymerization. Existing SIPs, such as polycarbamates,[1a, 2] polycarbonates,[3] poly(benzyl ether)s,[4] polyphthalaldehydes,[5] and polyglyoxylates,[6] mainly rely on nucleophilic/anionic depolymerization mechanisms including quinone methide elimination, cyclization and elimination of five-membered heterocycles, and hemiacetal fragmentation (Scheme 1A).[7] However, with a few notable exceptions,[4a, 8] these nucleophilic/anionic depolymerization mechanisms often result in the high sensitivity of these SIPs to even mild acidic/basic conditions, as well as slow and incomplete depolymerization.[9] Furthermore, the highly reactive intermediates generated during the ionic/nucleophilic depolymerization, such as quinone methides, can lead to undesirable side reactions with nucleophiles.[1b]

Since first reported by Katz et al,[10] enyne metathesis cascade reactions have emerged as powerful approaches to construct complex cyclic structures from linear precursors in synthetic organic chemistry[11] and chemical biology.[12] Earlier works by Choi,[13] Gutekunst,[14] Hawker,[14a] and Kilbinger,[15] have demonstrated the high efficiency of ruthenium (Ru)-catalyzed enyne metathesis cascades in chain-growth polymerization, polymer chain-end modification, and *in situ* initiator generation for ring-opening metathesis polymerization (ROMP, Scheme 1B). However, to the best of our knowledge, enyne metathesis cascade reactions have not previously been used to enable the depolymerization of synthetic polymers. Herein, we envision that a novel class of enyne SIPs can be designed to enable consecutive metathesis cascade-triggered depolymerization with high efficiency. Our SIP design entails a backbone structure consisting of repeating 1,6-enynes, such that the propagating Ru-carbene intermediate can undergo consecutive *5-exo-dig* and *5-exo-trig* cyclizations to eliminate a 1,1'-bicyclopentene derivative and regenerate the Ru carbene (Scheme 1C). The propagation of this enyne metathesis cascade reaction along the

Scheme 1. Development of the Enyne Self-Immolative Polymer

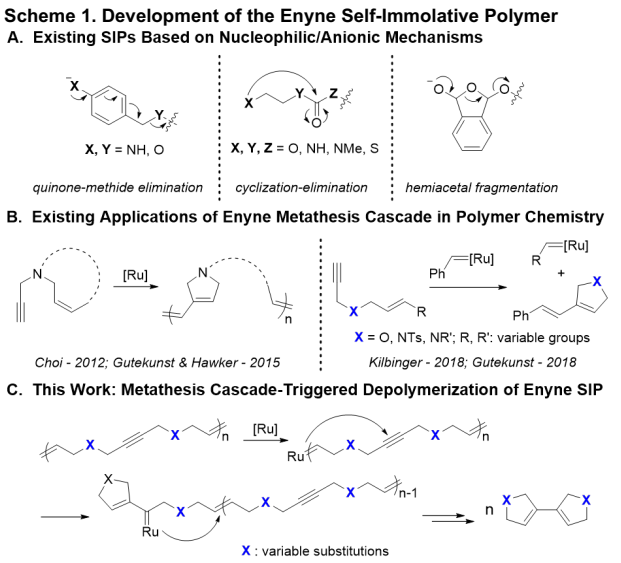

SIP backbone would lead to head-to-tail depolymerization. Fundamentally distinct from existing SIPs, our design involves no nucleophilically labile functional groups. Also, unlike the depolymerization of polycycloolefins (*e.g.*, polycyclopentene),[16] which is the reverse reaction of ROMP at the thermodynamic equilibrium, the enyne metathesis cascade-triggered depolymerization is irreversible, as the endocyclic trisubstituted alkenes in the 1,1'-bicyclopentene derivatives generated by the depolymerization are less-reactive to Ru catalysts.[17]

Our investigation began by studying a series of model compounds **1**–**7** capable of the enyne metathesis cascade reaction (Scheme 2). These model compounds consist of two fused 1,6-enyne structures, such that the adjacent alkenes and alkynes are separated by a –CH_2–X–CH_2– spacer, where X is a variable functional group that provides the steric buttressing effect[18] for the metathesis cascade cyclization triggered by third-generation Grubbs catalyst (**G3**). The variable X group also helps to improve the solubility of the model compounds. Except **5**, the reactions of model compounds **1**–**6** were found to proceed efficiently in the presence of 3 mol% **G3** in dichloromethane (DCM) or tetrahydrofuran (THF) at room temperature. The reactions reached quantitative conversions to afford the corresponding 1,1'-bicyclopentene derivatives **8**–**13** in high yields over 30 minutes (Scheme 2A). Likely due to the weak buttressing effect of the acetyl group, compound **5** only achieved 47% conversion under the same conditions. These observed reactivities of the enyne metathesis cascade reactions are consistent with previous reports by Grubbs *et al.*[19] and Nolan *et al.*[20] In contrast, although terminal alkynes are also known to initiate enyne metathesis, only 10% conversion was achieved to generate **14** when **7** was subjected to the same reaction conditions (Scheme 2B). The slow reaction of **7** was attributed to the lower reactivity of the vinyl carbene compared to the alkylidenes formed in **1**–**6** (Scheme S1).[17] Taken together, the model compound studies suggested that enyne structures with bulky substitutions could

Scheme 2. Enyne Metathesis of Model Compounds

A. Model compounds with terminal alkenes

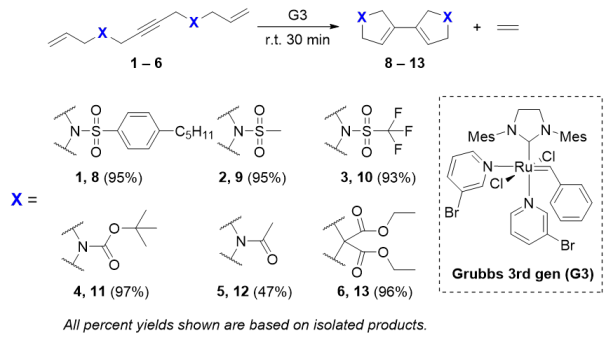

All percent yields shown are based on isolated products.

B. Model compound with terminal alkynes

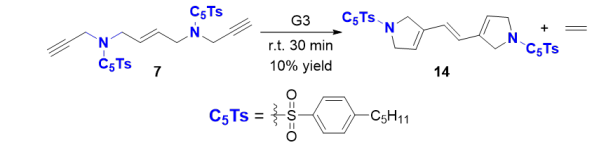

undergo efficient metathesis cascade reactions, and that terminal alkenes offer better reactivity compared to terminal alkynes.

Encouraged by these promising results, we attempted to prepare enyne SIPs via polycondensation. We chose X = *p*-pentyl-*N*-benzenesulfonamide as the spacer within the 1,6-enyne structure due to the high reactivity and excellent solubility of model compound **1**. Two distinct polycondensation approaches, AB-type and AABB-type, were explored. Retrosynthetic analysis of the target SIP gave rise to a bromosulfonamide enyne monomer **15** for the AB-type polycondensation, or a disulfonamide alkyne monomer **16** and

Table 1. Enyne SIPs via Polycondensation[a]

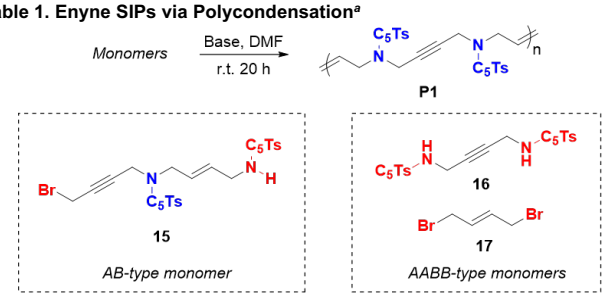

Entry	Monomer	Base	M_n(kg·mol^{-1})[b]	$Đ$[b]
1[c]	**16+17**	DBU	1.3	1.45
2[c]	**16+17**	NaH	1.2	1.50
3	**16+17**	TMG	1.2	1.20
4	**16+17**	K_2CO_3	1.8	1.50
5[c,d]	**16+17**	K_2CO_3	1.9	1.33
6	**16+17**	Cs_2CO_3	34.2	1.56
7[e]	**15**	Cs_2CO_3	1.5	1.46
8[f]	**16+17**	Cs_2CO_3	10.5	1.21

[a]Polymerization conditions: under air for 20 h, 4 eq. base. All polymerizations reached over 95% conversion as determined by crude ^{1}H NMR. Initial monomer concentration $[M]_0$ = 1.0 mol·L^{-1}. [b]Molecular weight (M_n) and dispersity ($Đ$) were determined by SEC analysis calibrated to polystyrene standards. For entries 6 and 8, M_n and $Đ$ are reported after precipitation in diethyl ether. [c]Reaction turned dark within 10 minutes. [d]The reaction was carried out at 80 °C. [e]Two equivalents of base were used. [f]Feeding ratio of **16**/**17** was 1.0/0.975. Polymerization time was 3.5 h and the resulting polymer was capped by 1 equiv. allyl bromide with respect to **16**.

trans-1,4-dibromo-2-butene **17** for the AABB-type polycondensation (Table 1; see Supporting Information for detailed procedures for monomer synthesis). Various inorganic and organic bases were investigated to optimize the reaction. All AABB polycondensations of **16** and **17** mediated by strong bases such as 1,8-diazabicyclo[5.4.0]undec-7-ene (DBU) and sodium hydride (NaH) resulted in a dark-colored complex mixture (Table 1, entry 1–2). In contrast, reactions mediated by 1,1,3,3-tetramethylguanidine (TMG) or potassium carbonate (K_2CO_3) proceeded with minimal color change; however, size exclusion chromatography (SEC) analysis showed that only products with low number average molecular weights (M_n) were obtained (Table 1, entry 3–4). Increasing the temperature to 80 °C did not improve M_n and also caused discoloration (Table 1, entry 5). Polymers with higher M_n were obtained when cesium carbonate (Cs_2CO_3) was used (Table 1, entry 6 and Table S1), which was attributed to the higher basicity and solubility of Cs_2CO_3 compared to K_2CO_3 in *N*, *N*-dimethylformamide (DMF). The low M_n cyclic oligomers fraction could be efficiently removed from the crude product by a simple precipitation in diethyl ether, yielding the linear polymer **P1** (Figure S1–S2). The synthetic procedure was readily scalable to prepare gram quantities of **P1**, indicative of the potential for further scaling up. Notably, AB polycondensation of monomer **15** only afforded low M_n oligomers (Table 1, entry 7), which was attributed to the high cyclization tendency of **15**. To our surprise, despite lacking terminal alkene chain ends, **P1** was able to undergo depolymerization, yielding 3,3'-bidihydropyrrole derivative **8** exclusively (Figure 1). However, a relatively high catalyst loading of 7 mol% **G3** (hereafter, catalyst loading is calculated with respect to the polymer repeating units) was necessary to achieve a complete conversion.

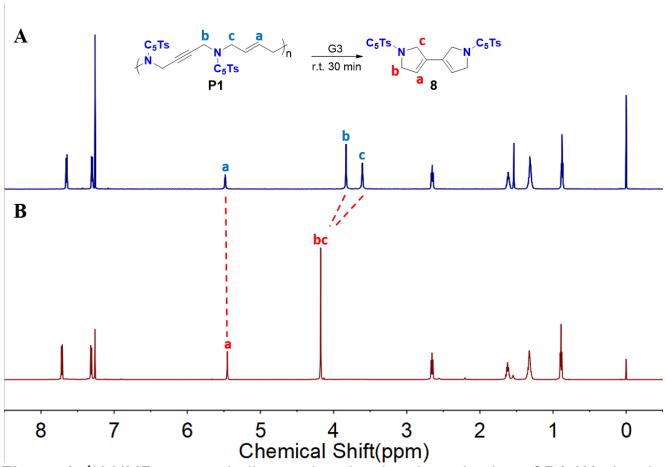

Figure 1. ^{1}H NMR spectra indicates that the depolymerization of **P1** (A) cleanly produced **8** (B).

The surprising depolymerization of **P1** prompted us to further investigate the role of the terminal alkene chain-end group in depolymerization. To this end, we devised an iterative exponential growth (IEG) route to synthesize discrete oligomers with well-defined terminal chain-end groups.[21] First, a bifunctional IEG monomer **18** carrying orthogonal acetyl (Ac) and *t*-butyloxycarbonyl (Boc) protecting groups was conveniently prepared by the Mitsunobu coupling of a monoBoc disulfonamide **19** and monoacetyl 1,4-butynediol (Scheme 3A). Selective deprotection of **18** at either ends produced two orthogonally monoprotected monomers, which were subsequently coupled via the Mitsunobu reaction to give the protected dimer **20**. Two more iterations of deprotection-coupling cycles afforded an octamer (Scheme 3B). Studies on the terminal alkene-capped dimers derived from **20** indicated that the oligomer

capped at the alcohol end underwent more efficient depolymerization compared to the one capped at the sulfonamide end. Both ends capped dimers were depolymerized more efficiently than the non-capped **20** (see Scheme S2 and Figure S3–S5 for detailed discussion). In light of this finding, the octamer was capped by a terminal alkene at the alcohol end to yield a discrete octameric enyne SIP **P2**, the structure of which was confirmed by NMR and mass spectrometry (Scheme 3C, Figure S6).

Scheme 3. IEG synthesis of discrete SIP oligomers

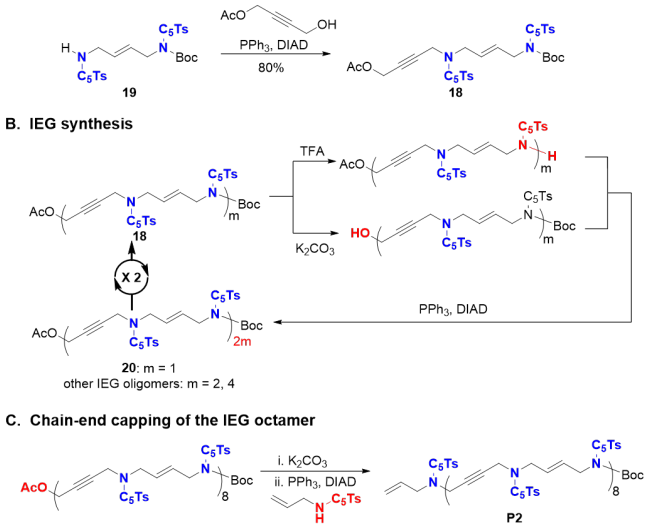

Depolymerization of **P2** was notably more efficient than **P1**, reaching full conversion over 40 minutes with 1.5 mol% **G3** (Figure S6). Monitoring the depolymerization of **P1** and **P2** by SEC revealed different modes of depolymerization. Notably, M_n of **P1** gradually decreased with increasing conversion (Figure 2A and Figure S7). In contrast, M_n of **P2** remained constant over the course of depolymerization (Figure 2B and Figure S8). We reasoned that the differences between **P1** and **P2** in the depolymerization efficiency and the mode of M_n evolution could be explained by how the reactions were initiated. Unlike the depolymerization of **P2** that always initiates from the terminal alkene chain end (Figure 2C), the depolymerization of **P1** is initiated when **G3** reacts with an internal alkene within the polymer backbone, generating a "leading" segment with a Ru-alkylidene chain end and a "lagging" segment with a 1,2-disubstituted alkene chain end (Figure 2D). While the leading segment depolymerizes in a head-to-tail fashion, the lagging segment must react with a second catalyst molecule to reinitiate. As a result, the depolymerization of the lagging segment is less efficient, requiring higher catalyst loading, and leads to a gradual decrease of M_n as the conversion increases. These results highlight the importance of the terminal alkene chain end in improving the efficiency of depolymerization for enyne SIPs.

To improve the depolymerization efficiency of the enyne SIPs prepared by polycondensation, we first prepared a polymer with predominantly sulfonamide chain ends by employing a feeding ratio of **16**:**17** = 1:0.975 (Table 1, entry 8). It should be noted that although **16** was in excess, the resulting polymer is unlikely to possess 100% sulfonamide chain ends due to the intrinsic lack of control over polycondensation. Indeed, further reacting this polymer with allyl bromide (1 equiv. with respect to **16**) produced an enyne SIP **P3** with 74% of the chains capped by at least one terminal alkene (Figure 3A, also see Figure S9 for detailed characterization methods). Despite **P3** being incompletely capped, its depolymerization was notably more efficient than uncapped **P1** (Figure S10), achieving complete depolymerization over 30 minutes in the presence of 3 mol% **G3**. Interestingly, although the amount of full-length **P3** rapidly decreased after initiation, M_n of the remaining polymer slightly increased initially before starting to decrease (Figure 3B). We reason that the short chains in **P3** were both more efficiently capped by the terminal alkene and may require fewer cascade steps to fully depolymerize, thus resulting in a more rapid consumption of these chains in the population (Figure S11).

P3 demonstrated excellent stability against spontaneous, uncontrolled degradation in strong acid, base, and nucleophiles. No structural changes were observed after **P3** was treated by trifluoroacetic acid, sodium hydroxide, benzyl amine, or 1-dodecanethiol. After these treatments, **P3** also maintained the same reactivity towards depolymerization (Figure S12–S15). Furthermore, we reason that the integration of the enyne SIPs with stimuli-responsive metathesis catalysts[22] would expand the utility of this technology in materials science. To this end, we incubated **P3** with a temperature-dependent catalytic system consisting of 3 mol% second-generation Grubbs catalyst (**G2**) and 3 mol% tributyl phosphite inhibitor.[23] **P3** was found to be stable when **G2** was inhibited at room temperature (Figure S16). Upon heating the system to 100 °C, the inhibition was reversed and the depolymerization proceeded with >95% conversion over just 95 seconds (Figure 3C and Figure S17). This result not only showcased the potential of the enyne SIPs as stimuli-responsive materials, but also suggested that efficiency of depolymerization could increase significantly at elevated temperatures.

In conclusion, a novel class of enyne SIPs capable of metathesis cascade-triggered depolymerization was developed. Examination of a series of model compounds identified the repeating 1,6-enyne motif with the *p*-pentyl-*N*-benzenesulfonamide spacer as the optimal backbone structure, which was readily incorporated into the SIPs via either polycondensation or IEG approaches. The resulting SIPs were stable in strong acid, base, or nucleophiles, and can undergo efficient depolymerization when triggered by metathesis catalysts. Investigation of the oligomers derived from the IEG route and polymers derived from the polycondensation route proved the importance of the terminal alkene for improving the efficiency of depolymerization. This work established a general approach to stimuli-responsive materials capable of controlled release of heterocyclic reagents with high efficiency and bio-orthogonality, laying the foundation for future applications in biosensing and drug delivery.

Acknowledgements

We thank T. Jayasundera for the help in NMR, and M. Domin for the assistance in MALDI-TOF. This work is supported by a CAREER award from the National Science Foundation (CHE-1944512) to J.N. and a Beckman Young Investigator Award to J.N. from the Arnold and Mabel Beckman Foundation.

Conflict of interest

The authors declare no competing financial interest.

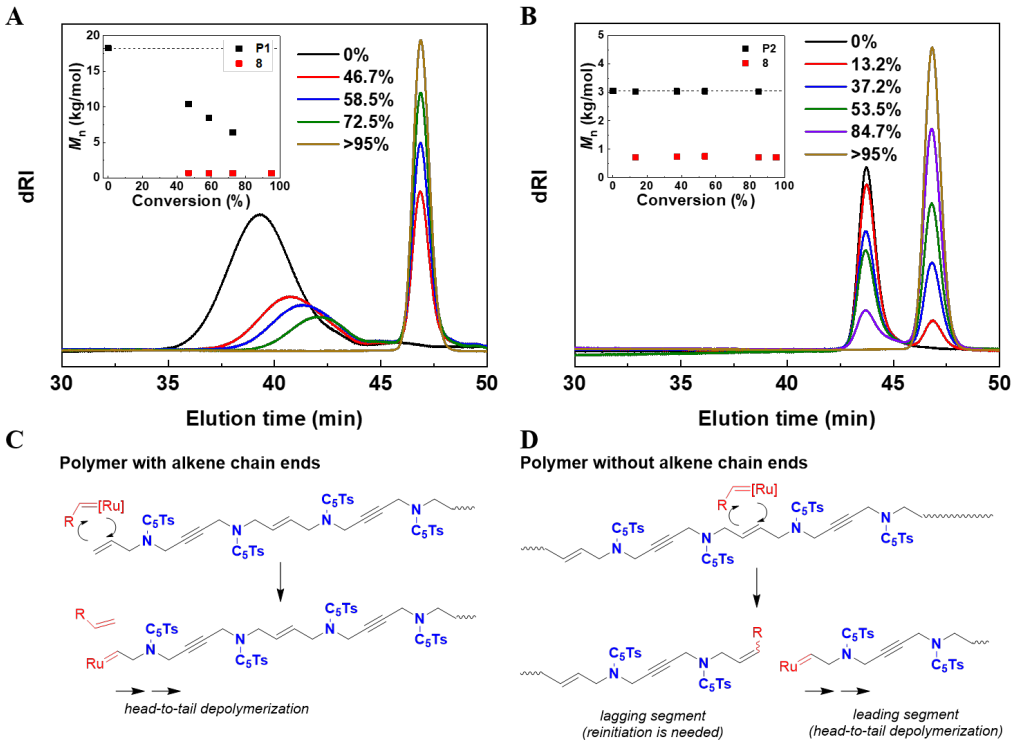

Figure 2. Depolymerization of **P1** and **P2**. (AB) Evolution of the SEC traces of **P1** (A) and **P2** (B). Insets: M_n with respect to conversion. (CD) Proposed depolymerization mechanisms of **P2** (C) and **P1** (D).

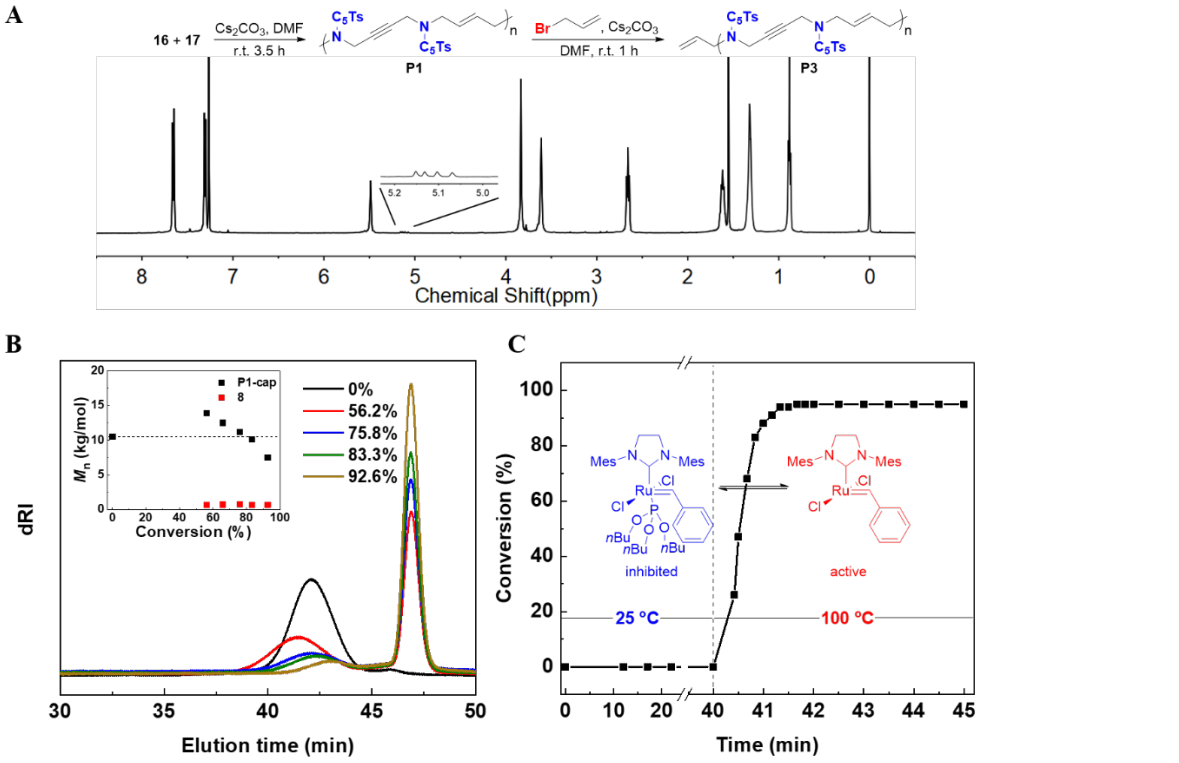

Figure 3. (A) Synthesis and ^{1}H NMR of **P3**. (B) Evolution of the SEC traces of the depolymerization of **P3**. Insets: M_n with respect to conversion. (C) The conversion-time plot of thermally responsive depolymerization of **P3**.

Keywords: Self immolative polymer • Enyne metathesis • Cascade reaction • Depolymerization • Stimuli-responsive materials

[1] a) A. Sagi, R. Weinstain, N. Karton, D. Shabat, *J. Am. Chem. Soc.* **2008**, *130*, 5434-5435; b) R. E. Yardley, A. R. Kenaree, E. R. Gillies, *Macromolecules* **2019**, *52*, 6342-6360; c) Y. Xiao, X. Tan, Z. Li, K. Zhang, *J. Mater. Chem. B* **2020**, *8*, 6697-6709; d) G. I. Peterson, M. B. Larsen, A. J. Boydston, *Macromolecules* **2012**, *45*, 7317-7328.

[2] A. P. Esser-Kahn, N. R. Sottos, S. R. White, J. S. Moore, *J. Am. Chem. Soc.* **2010**, *132*, 10266-10268.

[3] a) S. Gnaim, D. Shabat, *J. Am. Chem. Soc.* **2017**, *139*, 10002-10008; b) Y. Xiao, Y. Li, B. Zhang, H. Li, Z. Cheng, J. Shi, J. Xiong, Y. Bai, K. Zhang, *ACS Macro Lett.* **2019**, *8*, 399-402.

[4] a) M. G. Olah, J. S. Robbins, M. S. Baker, S. T. Phillips, *Macromolecules* **2013**, *46*, 5924-5928; b) K. Yeung, H. Kim, H. Mohapatra, S. T. Phillips, *J. Am. Chem. Soc.* **2015**, *137*, 5324-5327.

[5] a) C. Aso, S. Tagami, *J. Polym. Sci., Part B: Polym. Lett.* **1967**, *5*, 217-220; b) J. A. Kaitz, C. E. Diesendruck, J. S. Moore, *J. Am. Chem. Soc.* **2013**, *135*, 12755-12761; c) C. E. Diesendruck, G. I. Peterson, H. J. Kulik, J. A. Kaitz, B. D. Mar, P. A. May, S. R. White, T. J. Martinez, A. J. Boydston, J. S. Moore, *Nat. Chem.* **2014**, *6*, 623-628.

[6] a) B. Fan, J. F. Trant, A. D. Wong, E. R. Gillies, *J. Am. Chem. Soc.* **2014**, *136*, 10116-10123; b) B. Fan, J. F. Trant, E. R. Gillies, *Macromolecules* **2016**, *49*, 9309-9319.

[7] A. Alouane, R. Labruere, T. Le Saux, F. Schmidt, L. Jullien, *Angew. Chem. Int. Ed.* **2015**, *54*, 7492-7509.

[8] A. M. DiLauro, S. T. Phillips, *Polym. Chem.* **2015**, *6*, 3252-3258.

[9] S. T. Phillips, A. M. DiLauro, *ACS Macro Lett.* **2014**, *3*, 298-304.

[10] a) T. J. Katz, S. J. Lee, M. Nair, E. B. Savage, *J. Am. Chem. Soc.* **1980**, *102*, 7940-7942; b) T. J. Katz, E. B. Savage, S. J. Lee, M. Nair, *J. Am. Chem. Soc.* **1980**, *102*, 7942-7944.

[11] M. Serra, E. Bernardi, L. Colombo, *Synthesis* **2020**, *53*, 785-804.

[12] a) J. B. Binder, R. T. Raines, *Curr. Opin. Chem. Biol.* **2008**, *12*, 767-773; b) V. Sabatino, T. R. Ward, *Beilstein J. Org. Chem.* **2019**, *15*, 445-468; c) V. Sabatino, J. G. Rebelein, T. R. Ward, *J. Am. Chem. Soc.* **2019**, *141*, 17048-17052.

[13] a) H. Park, T. L. Choi, *J. Am. Chem. Soc.* **2012**, *134*, 7270-7273; b) H. Park, H. K. Lee, T. L. Choi, *J. Am. Chem. Soc.* **2013**, *135*, 10769-10775; c) A. Bhaumik, G. I. Peterson, C. Kang, T. L. Choi, *J. Am. Chem. Soc.* **2019**, *141*, 12207-12211.

[14] a) W. R. Gutekunst, C. J. Hawker, *J. Am. Chem. Soc.* **2015**, *137*, 8038-8041; b) T. Q. Zhang, L. B. Fu, W. R. Gutekunst, *Macromolecules* **2018**, *51*, 6497-6503; c) X. Sui, T. Zhang, A. B. Pabarue, L. Fu, W. R. Gutekunst, *J. Am. Chem. Soc.* **2020**.

[15] a) S. Pal, F. Lucarini, A. Ruggi, A. F. M. Kilbinger, *J. Am. Chem. Soc.* **2018**, *140*, 3181-3185; b) M. Yasir, P. Liu, I. K. Tennie, A. F. M. Kilbinger, *Nat. Chem.* **2019**, *11*, 488-494.

[16] W. J. Neary, J. G. Kennemur, *ACS Macro Lett.* **2018**, *8*, 46-56.

[17] S. T. Diver, A. J. Giessert, *Chem. Rev.* **2004**, *104*, 1317-1382.

[18] N. Choony, N. Kuhnert, P. G. Sammes, G. Smith, R. W. Ward, *J. Chem. Soc., Perkin Trans.* **2002**, 1999-2005.

[19] S. H. Kim, N. Bowden, R. H. Grubbs, *J. Am. Chem. Soc.* **1994**, *116*, 10801-10802.

[20] H. Clavier, A. Correa, E. C. Escudero-Adan, J. Benet-Buchholz, L. Cavallo, S. P. Nolan, *Chem-Eur. J.* **2009**, *15*, 10244-10254.

[21] a) J. C. Barnes, D. J. Ehrlich, A. X. Gao, F. A. Leibfarth, Y. Jiang, E. Zhou, T. F. Jamison, J. A. Johnson, *Nat. Chem.* **2015**, *7*, 810-815; b) F. A. Leibfarth, J. A. Johnson, T. F. Jamison, *Proc. Natl. Acad. Sci. U.S.A.* **2015**, *112*, 10617-10622.

[22] A. J. Teator, C. W. Bielawski, *J. Polym. Sci. Pol. Chem.* **2017**, *55*, 2949-2960.

[23] I. D. Robertson, L. M. Dean, G. E. Rudebusch, N. R. Sottos, S. R. White, J. S. Moore, *ACS Macro Lett.* **2017**, *6*, 609-612.